An Analysis of the Optical Features of the Near-Bottom and Bottom Nepheloid Layers in the Area of the Scotian Rise

RICHARD W. SPINRAD AND J. RONALD V. ZANEVELD

School of Oceanography, Oregon State University, Corvallis, Oregon 97331

Profiles of light transmission versus depth have been studied in the region of the Scotian Rise of the North Atlantic at bottom depths between 4900 and 5000 m. A component model has been developed and consists of three components of transmission which can be combined to duplicate accurately any given transmission profile. Two of the components are shown to be representative of several basic phenomena: the particle concentration within a uniform flow and the separation of a benthic nepheloid layer. In the case of a uniform flow it is the relative magnitudes of settling and eddy diffusion which determine the shape of the transmission profile. Separation of the benthic nepheloid layer was inferred to be caused by an occasional cross-slope velocity component. The physical interpretation of the third component was ambiguous. Eulerian and Lagrangian transformations of the data show that benthic 'storms' that were detected at one location and time appeared nearly identical at a later time downstream and that benthic 'storms' can be detected over a large distance. Distance and time scales obtained from these transformations show the area of the Scotian Rise to be one characterized by bottom 'storms' which keep their general form over periods of at least 2 weeks and for distances traveled of at least 400 km.

INTRODUCTION

Profiles of light transmission (at 660-nm wavelength) were made as part of the high-energy benthic boundary layer experiment (HEBBLE) on the Scotian Rise off New England (Figure 1). While data were collected at 44 stations, this work will concentrate on the information obtained from stations having bottom depths between 4900 and 5000 m. This depth range corresponds to the zone in which bottom photographs, current meters, transmissometers, and sediment traps all indicated the highest levels of near-bottom turbulence [*Hollister et al.*, 1980; C. D. Hollister et al., personal communication, 1982]. The stations within this zone are indicated on Figure 1.

The use of the light beam transmissometer as a tool in particle detection and quantification in the area of the Scotian Rise has been verified in previous work [*Spinrad*, 1982; *Spinrad and Zaneveld*, 1982]. It was shown that with measurements of light tranmission the particle volume concentration could be measured accurately, in situ. I. N. McCave (personal communication, 1982) verified this with additional research in the same area. The correlation of particle concentration P (in parts per billion volume concentration) to transmission for the nonsurface waters of the Scotian Rise is given by

$$c = 1.756 \times 10^{-3}P + 0.465$$
$$r^2 = 0.93$$
(1)

where c is the beam attenuation coefficient (units of m^{-1}) defined as the internal attenuance of an infinitesimally thin layer of the medium normal to the beam divided by the thickness of the layer [*Jerlov*, 1976]. Also

$$c = -\frac{1}{d}\ln T$$
(2)

where T is the fraction of transmitted light or transmission and d is the pathlength (1 m in this case).

The transmissometer has an error limit of less than 0.5% transmission over the thermal range of 0°C to 25°C [*Bartz et al.*, 1978]. In the nearly isothermal environment under consideration here the error is significantly less (~0.1%).

The major question asked in this study is: what is the nature of the benthic nepheloid layer in the HEBBLE area as determined from optical measurements? The temporal and spatial scales of formation of benthic turbidity 'storms' will be analyzed as well as the stability over time and space of these phenomena. The physical systems we thought were responsible for the structure of the particle concentration will be discussed. Several recurrent small-scale (10^2 m) and large-scale (10^2 km) optical features will be presented, and their roles in the overall scheme of sediment transport will be discussed.

COMPONENT ANALYSIS

By means of the correlation of beam transmission and particle volume concentration outlined previously the transmission profiles may be used to provide the volume concentration profile. While no two transmission profiles that were obtained were identical, it has become apparent that there are only a few general types of profiles seen in the HEBBLE area. All of the profiles may be arbitrarily broken down into combinations of three well-defined components. Two of these components can be readily interpreted in physical terms to yield the particle profiles. The physical interpretation of the third component is not obvious at present. Thus, by considering all of the transmissometer profiles as combinations of the same components the interactions of these physical systems on the Scotian Rise may be better understood. It would also be possible to consider each profile individually by 'smoothing' the data and reducing each transmission value to a particle concentration. Such a method might be inherently more precise for each unique transmission profile, but it would be of little use in the consideration of the overall picture of how the physical systems of sediment transport interact within the area.

The three model components were derived numerically from the transmission profiles using a least squares regression. The components are shown in Figures 2a–2d. Respec-
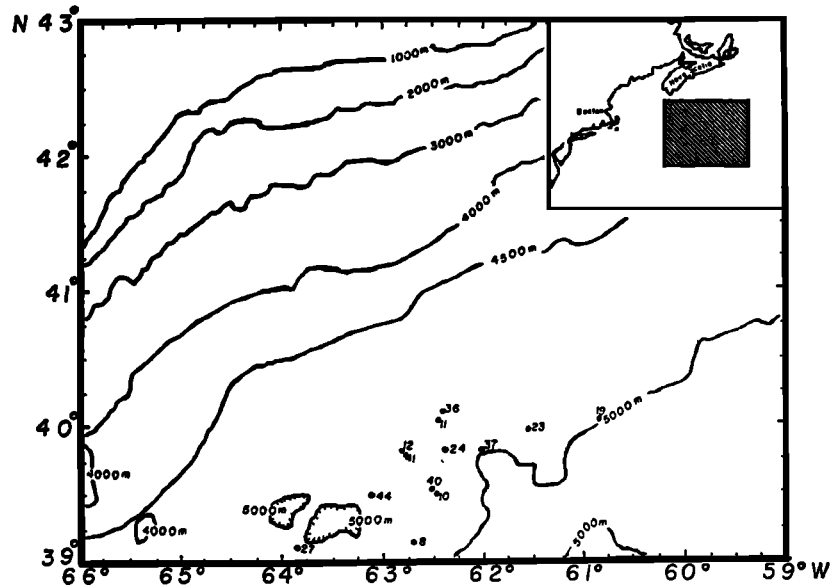
Fig. 1. Bathymetry and station locations for experimental area.

tively, these profiles are defined as follows:

$$T = A\xi + B \tag{3a}$$

$$T = A \sin B\xi + D \tag{3b}$$

$$T = A \sin^2 B\xi + D \tag{3c}$$

where ξ is a nondimensional distance above the bottom given by z/h (h is the height of the flow zone; z is positive upward) and A, B, and D are constants determined by the shape of the specific profile under consideration. The coefficients in (3a)–(3c) were derived numerically from the transmissometer profiles. Equations (3a)–(3c) express transmission and therefore beam attenuation coefficient as a function of height above bottom; (1) expresses particle concentration as a function of beam attenuation coefficient and therefore transmission. Thus, combining (1), (2), and (3a)–(3c), respectively, will yield expressions of concentration as a function of altitude as follows:

For (3a)

$$P = -265.1 - 569.5 \ln (A\xi + B)$$

For (3b)

$$P = -265.1 - 569.5 \ln (A \sin B\xi + D)$$

For (3c)

$$P = -265.1 - 569.5 \ln (A \sin^2 B\xi + D)$$

when the path length d is 1 m.

These components will be referred to as components I–III, respectively (that is, component I corresponds to (3a); component II corresponds to (3b), etc.). Component III never occurs by itelf but is found in the data as a linear addition to either component I or II. In actuality any observed profile may be considered to be a juxtaposition or superposition of these components.

Component I (linear) basically represents a system of particles within a uniform, steady flow. This is especially apparent in the case when T is nearly constant with altitude

($|A| \ll 1$). Such is the case in the bottom boundary layer for several stations. As the transmission values increase with altitude, the profile characterized by component I is representative of a system in which particle settling has begun. If an initially well-mixed polydisperse particle mixture is allowed to settle, the continuous range of particle settling velocities will produce a smooth transition from a low concentration of particles near the top to a high concentra-
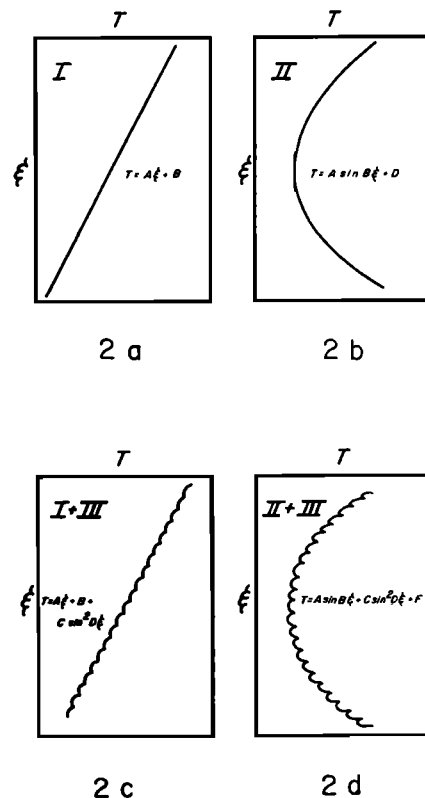

Fig. 2. Components of transmission profiles as used in data analysis (see text for definition of ξ).

tion below at a given time. If a simplified eddy diffusion-settling model is considered for a steady, uniform flow, the solution for particle concentration is of the form

$$P(\xi) \propto \xi^{-b}$$

[e.g., *Shepard*, 1963; *Raudkivi*, 1967; *Smith and McLean*, 1977], where b is a coefficient that depends on particle settling velocity and magnitude of the flow. *Raudkivi* [1967] has shown that by varying 'b,' the ratio of the relative magnitudes of settling velocity and eddy diffusion, one can obtain particle concentration profiles which agree in appearance with those of component I. Using a series expansion for the solution above, one finds that to first order the particle concentation is characterized by a logarithmic profile:

$$\xi^{-b} \simeq 1 - b \ln \xi$$

so $P \propto \ln \xi$, provided b is small (as when the vertical eddy diffusion coefficient is relatively high).

This is in direct agreement with the profile of particle concentration that is obtained from (3a) in which it is seen that for a linear transmission profile,

$$P = -265.1 - 569.5 \ln (A\xi + B)$$

or

$$P \propto \ln \xi$$

Thus it is apparent that, in general, component I repre-
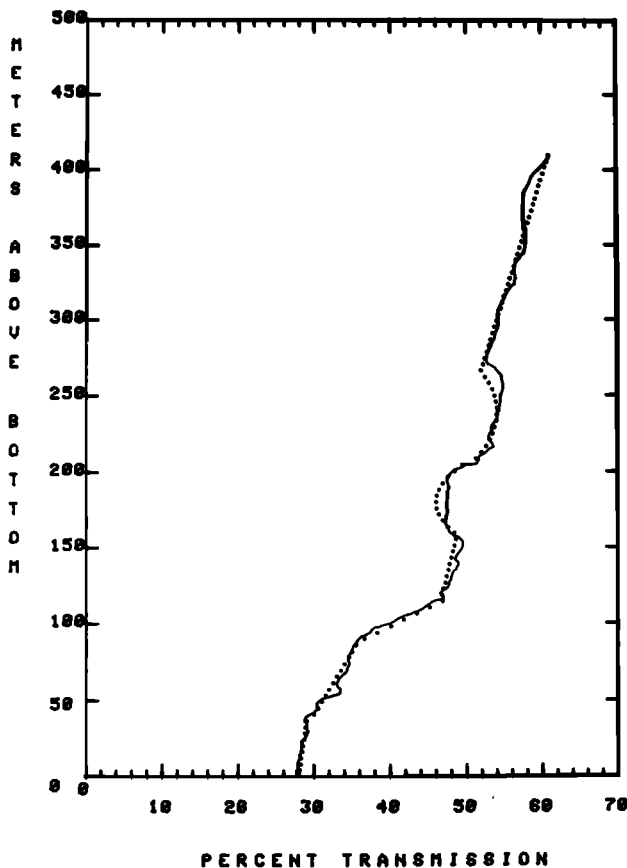
STATION 23

Fig. 3. Comparison of actual transmission profile (thin solid line) and component model (heavy dotted line) for station 23.
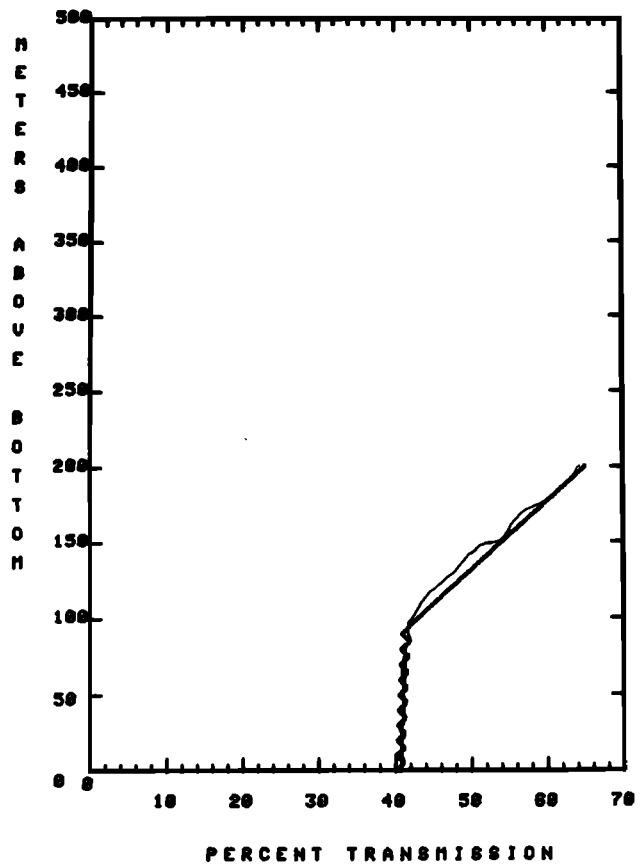
STATION 44

Fig. 4. Comparison of actual transmission profile (thin line) and component model (heavy line) for station 44.

sents a horizontally uniform system in steady state. The slope of the transmission profile is indicative of the relative magnitudes of particle settling velocity and vertical eddy diffusion. The resemblance of profiles derived from models of steady, uniform eddy diffusion/settling, and the transmission profiles shows that wherever component I exists the system is probably dominated by a uniform current of nonvarying turbulence in which particle settling produces a logarithmic profile of particle concentration. The logical extension of this physical system occurs when the transmission value is nonvarying with altitude. In such a case, particle settling is minimized, probably by relatively high turbulence. In fact, using the previous argument, as $b \rightarrow 0$, $P \rightarrow 1$, a value which is constant over depth. There is no indication in the transmission profiles that the slope is at all affected by or dependent on the degree of turbidity. Overall, component I appears to characterize a system in which there is little variability in vertical activity (after the initial homogenization, of course). The system may be well mixed initially and then settling and eddy diffusion become the dominant processes.

Component II (sinusoidal) is a transient feature which was detected above the bottom at four stations (23, 24, 37, and 41). While Figure 2b depicts component II as a smoothly varying function of moderate amplitude and wavelength, the actual data profiles varied considerably from sharp, narrow peaks to broad, low-amplitude transmission minima.

The transmission profiles and temperature profiles will
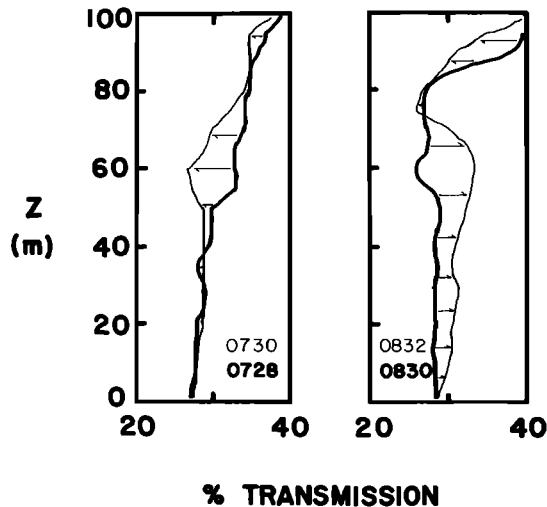
% TRANSMISSION

Fig. 5. Transmission profiles taken consecutively at station 23.

indicate that the water masses of component II have characteristics similar to the water masses at the bottom. Intermediate particle maxima have been detected elsewhere in the deep ocean [*Armi and D'Asaro,* 1980] and have been traced back to benthic boundary layers where there is a relatively fast current and rough topography leading to increased vertical turbulence. The sinusoidal band develops as a detachment from the bottom nepheloid layer and may exist over a distance of tens of kilometers. Such a process also occurs at the shelf break where detached benthic layers form to become intermediate nepheloid layers over the continental slope [*Pak et al.,* 1980*b*]. The relative cleanliness of the waters above and below the intermediate band suggest that detachment from the benthic boundary layer is the most likely explanation for the appearance of component II.

Component III only occurs at a very few stations, and the physical explanation for it is not obvious. When the feature occurs, it is characterized by uniform transmission increases and decreases of the order of 1–2% over a vertical distance of approximately 5 m (this may be considered significant since the accuracy of the instrument is roughly 0.1%). The altitude of a particular maximum or minimum of transmission may vary over a short period of time. There are no concurrent anomalies in the temperature profile to indicate anything other than a uniform water mass within the zones described by component III. These zones are roughly 70–100 m thick, and they are limited to regions where the transmission is roughly between 35 and 50% (turbid but not exceptionally so). The phenomenon defined by component III may be a figment of the trajectory of the instrument. The path of the instrument through the water column may, in fact, be the explanation behind the appearance of these apparent particle laminae.

To identify positively the process which is the driving force behind the appearance of component III would require extensive measurements with moored and profiling transmissometers as well as current meters.

Small-Scale Observations

The profiles were decomposed into segments, each having a form characterized by one of the components. The number of components in a profile varied from one to seven with a mean of three. The term *h* was determined as being the

altitude at which the transmission reached a steady, high value. This height varied from 60 to 410 m above bottom with a mean value of 180 m. Figures 3 and 4 show examples of the agreement between the data and the numerical component model using the parameters given in the table for two characteristic profiles (Figure 3 represents a complex profile, while Figure 4 is a simpler one).

Component I was by far the most prevalent component found in the transmission profiles. Every station but one (number 37) contained at least one section of the profile defined by component I. Of the total of 42 components observed in 13 profiles, 27 were component I. In Figure 3, component I is used for defining all of the features of the profile except for the two sections between 155 and 265 m above bottom. Similarly, component I is shown in Figure 4 in the section above 90 m above bottom.

As discussed previously, component I is characteristic of a system of particles within a steady turbulent flow. The slope of the linear component was shown to be reflective of the relative magnitude of settling velocity and eddy diffusion (with a higher value of the slope corresponding to higher relative eddy diffusion). The mean value of the slope (A in (3a)) was 0.34, but the standard deviation of 0.59 demonstrates that there is wide variability in the slope of the transmission profile. A negative value of the slope was detected at two stations (stations 10 and 11), and although small in magnitude (−0.02 and −0.11, respectively), it indicates that there is occasional vertical particle transport sufficient to yield small increases in turbidity with altitude above bottom in the form of component I.

At two stations (23 and 24) the sinusoidal decrease in transmission characterized by component II was accompanied by a small sinusoidal increase immediately above it. This phenomenon was observed only at these two stations, which also happen to be the stations with the most complex structure. The 'positive sine' transmission profile (i.e., $A >$ 0) always occurred with the 'negative sine' transmission profile directly below it. This structure may represent a complication of the simple model of a detached benthic layer or it may be an artifact of the empirical model. The exact mechanism for such a consequence is open for speculation.

At one station the process involved in the development of component II was actually detected from the onset, and the
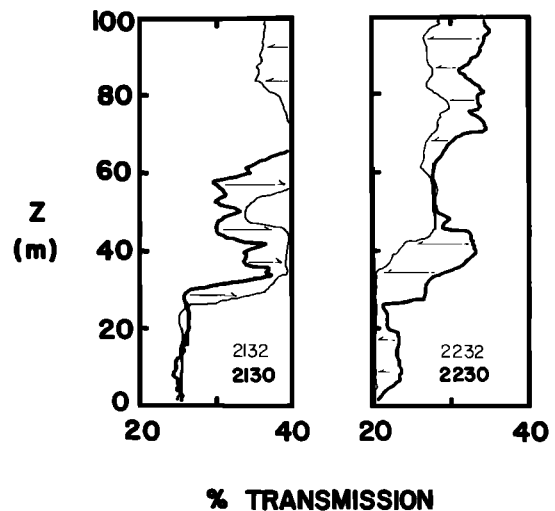

% TRANSMISSION

Fig. 6. Transmission profiles taken consecutively at station 24.

profiles obtained present dramatic evidence of this growth process. Figure 5 shows two series of two transmission profiles taken consecutively at station 23. The times for each cast are shown on the figure. In the first two casts labeled 0728 and 0730 there was little change in the transmission below about 50 m. The decrease in transmission at 50–60 m above bottom suggests that a cross-slope horizontal process is involved in bringing in suspended matter. The second series of casts at 0830 and 0832 clearly shows the transmission decreasing with time at 70–100 m above bottom and increasing in the water column below 70 m. This strongly suggests that vertical processes were involved in raising the particulate maximum that had been developed an hour earlier to a higher altitude above bottom. The detached nepheloid layers are not necessarily stable since they are physically unbounded and they represent significant fluctuations from the local conditions. In fact, where component I was seen to exist repeatedly over several casts, the features of component II at a given location changed dramatically over periods of less than 1 hour. Such drastic fluctuations and variations in the intermediate nepheloid layer are shown in Figure 6, which depicts a similar 'time series' of profiles for station 24. Figure 6 also indicates a vertical transport of particles above the near-bottom zone of constant turbidity in the first hour. The second hour is characterized by a nearly uniform (with depth) decrease in transmission. This may be a consequence of large-scale horizontal transport of turbid benthic clouds, as are described in the following section.

Figures 7a–7c show the temperature and transmission profiles at stations 8, 19 and 40, respectively. These three profiles demonstrate that when they are well mixed, the bottom waters are characterized by a temperature decrease and a coincident increase in turbidity. A similar observation was made in other benthic regions by *Biscaye and Eittreim* [1974]. *Weatherly et al.* [1980] have described the bottom nepheloid layer in this region as a cold, murky filament of water. The observation that the appearance of component II in the transmission profiles coincides with a drop in temperature in nearly all cases provides evidence of the benthic origin of component II. The most dramatic example of this is shown in Figure 8, which shows the transmission and temperature profiles for station 41. The near-bottom component II shows a decrease in transmission of roughly 15% from the immediate value. Concomitant with this is a drop in temperature of 25 m°C.

Component III only appears in several stations; these are stations which, in all other respects (temperature, pressure, turbidity, salinity), are similar to many other stations. In one slightly shallower station (CTD station 34; bottom depth 4880 m), component III was detected on the first downcast, the first upcast, and the second downcast. However, on the second upcast the turbidity was greatly decreased (from a minimum of 32–35% on the three earlier casts to a minimum of 53%), and component III was no longer present.

LARGE-SCALE OBSERVATIONS

In order to make sensible large-scale observations of the optical data on the Scotian Rise, some type of normalization must be used to bring the information into a cohesive form. One means of doing this is to use available velocity data to transform the time or location of each station in order to simulate a data set that is purely temporally or spatially variant. The data set as it presently stands contains the
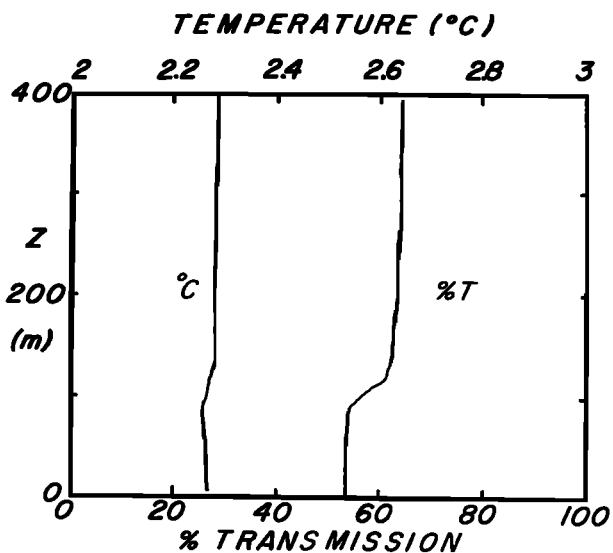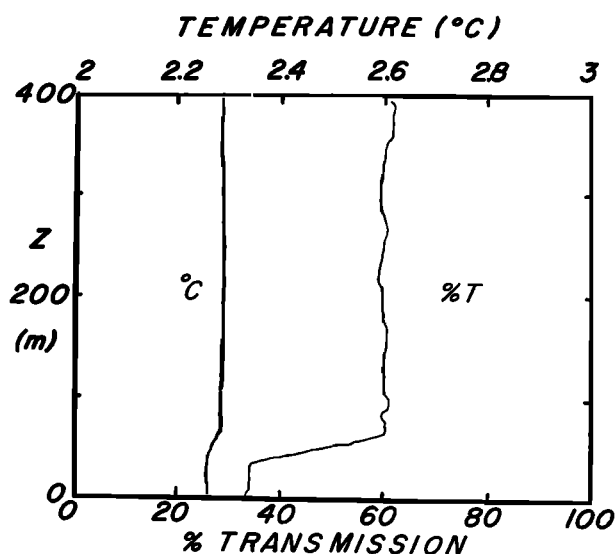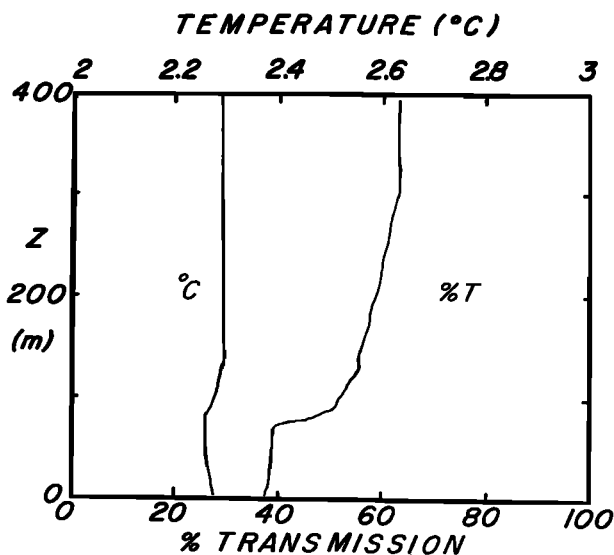

Fig. 7a

Fig. 7b

Fig. 7c

Fig. 7. Transmission and temperature profiles taken at (a) station 8; (b) station 19; (c) station 40.
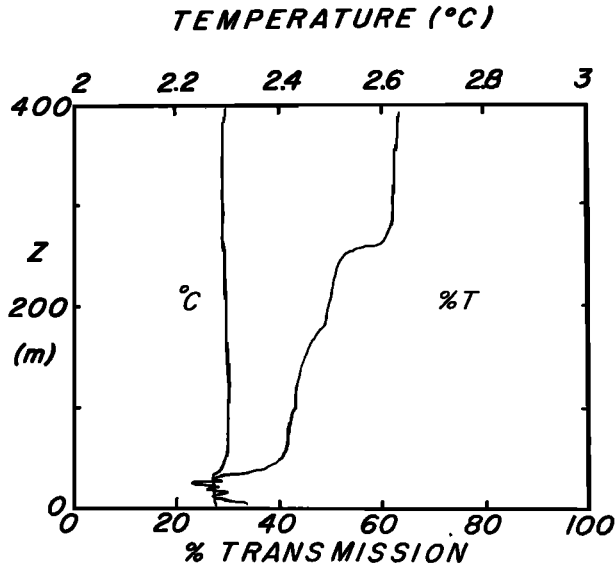
Fig. 8. Transmission and temperature profiles taken at station 41.

effects of both extensive temporal and spatial variations. It is most instructive to separate these two effects and study the large-scale system as it appears at a fixed point in space (Eulerian transformation) and as it appears over an area at a fixed time (Lagrangian transformation).

The first transformation performed was the Eulerian one relative to station 11. Station 11 was chosen as the reference site since the bottom ocean monitor (BOM) was located nearby. The BOM is a moored platform containing a light transmissometer, a nephelometer, and an Aanderaa current meter. Thus, by using station 11 as the reference, the time series obtained can be compared to the time series from the BOM. A current meter was deployed near station 11 at a depth of 4935 m (50 m above bottom) by M. J. Richardson of Woods Hole Oceanographic Institution. The current meter data obtaind for the period from September 13, 1979, to September 24, 1979, indicate a slow increase in current velocity from about 5 cm/s on September 13 to 40 cm/s on September 19 followed by a period of steady flow followed

by a sudden decrease on September 23. The flow was to the southwest and roughly parallel to the bottom contours. Using the assumption that the flow extends over a wide swath ($\sim 10^2$ km) as claimed by *Weatherly et al.* [1980] and using the velocity data outlined above coupled with the location of each station, the 'bottom time' (i.e., time at which the first downcast was complete) for each station was transformed to the time at which the water at that station would have been detected at or directly upslope or down-slope from station 11. Figure 9a shows the resultant time-based plot of transmission obtained from the Eulerian transform for depths of 0 m, 100 m above bottom and 200 m above bottom. Also shown is the plot of transmission from the moored bottom ocean monitor. The mean error in transmission between the BOM and the 0-m transmissometer plot is less than 10% transmission. This error may be ascribed to small local turbidity fluctuations. Figure 9b shows the time series of the depth profiles of transmission. The most obvious feature of Figures 9a and 9b is the excellent qualitative agreement between the time series as obtained from the transformation and the actual in situ time series. Both the BOM and the transformed profiles indicate a strong benthic storm between September 18 and September 20, Similarly, a weaker (i.e., less turbid) storm was detected by both techniques between September 22 and September 23. It is important to note that the BOM plot is continuous over time, while the transmissometer transformations are instantaneous. Thus, the actual fit of the two data sets may in fact be even better at the times in between those indicated for each transmissometer profile station.

The observation that is implicit from a study of Figures 9a and 9b is that benthic 'storms' on the Scotian Rise are large scale (temporally) and relatively invariant over a period 2–3 weeks. The fact that the transformation corresponds well with the BOM data indicates that the storm that was detected near September 19 at the BOM was the same storm that was detected at station 27 on September 23. In addition, the temporal transformation was performed for data collected over a period of some 19 days. Since this transformation agrees with the fixed-point data, one must conclude that the processes detected in this area occur as well-defined phe-
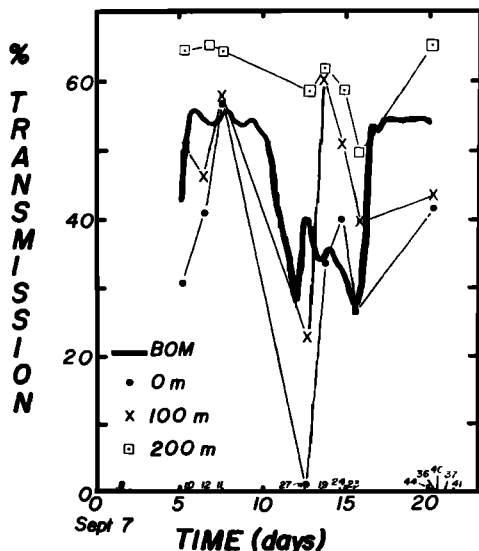

Fig. 9a. Time series of transmission at three depths and for the moored bottom ocean monitor (small numbers are station numbers).
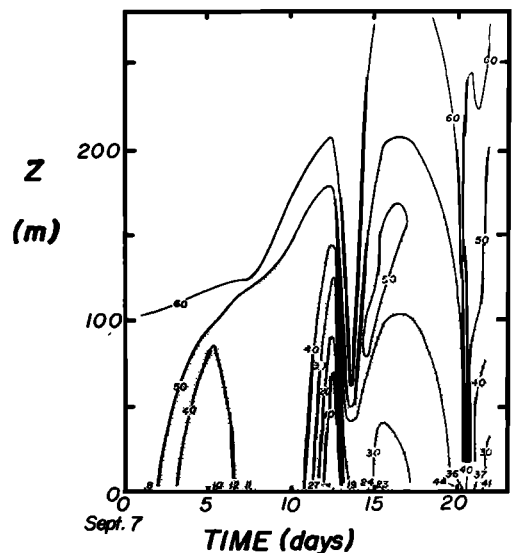

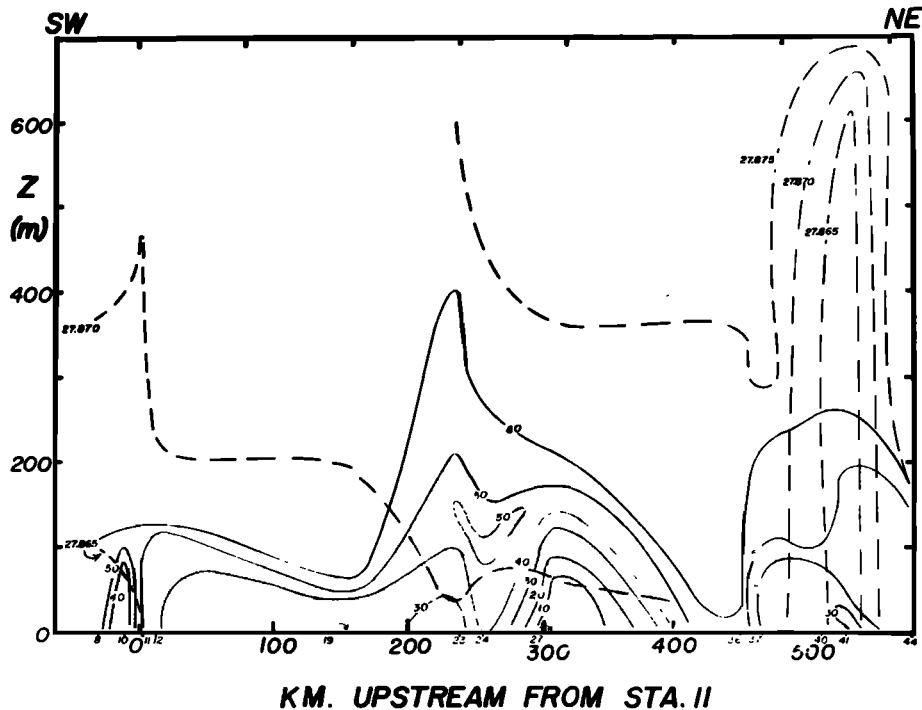Fig. 9b. Time series contours of transmission.

Fig. 10. Section of transmission and σ_t data (small numbers along distance scale are station numbers; dashed lines are σ_t data).

nomena over time periods of 2–3 weeks. The general form of the storm remains unchanged, and the record of activity at one station is consistent with the record at a distant station when the appropriate temporal transformation is made based on velocity information. The major optical features detected in these stations remain relatively unchanged as they are transported downstream over periods of at least 2 weeks.

The logical extension of this observation is an analysis of spatial transformations. A Lagrangian transformation was performed upon the data set. This was done in a manner nearly identical to that described previously with respect to the Eulerian transformation. However, in this case the unknown variable for which a solution was sought was the change in distance from station 11, not the change in time. The same velocity profile as previously described was used. The actual time at which each station was taken was compared to the time for station 11. The time difference between the two stations was applied to the velocity data to determine where the water sample from a given station would have been located at the time of measurement of station 11. Again, flow was assumed to be parallel to the contours toward the southwest.

Figure 10 presents a section view of the transmissometer data. The most obvious feature of the figure is the length scale along the section. The result of applying the Lagrangian transformation to the data has been to stretch effectively the length of the section from roughly 240 km (see Figure 1) to almost 640 km. Thus, the effects that were described previously as being large scale temporally can now also be considered to be large scale spatially. The fact that the Eulerian transformation yielded good results, coupled with the consequent large size scale induced by the Lagrangian transformation indicates that the phenomena detected on the Scotian Rise travel over distances of hundreds of kilometers while keeping their basic optical structure.

Also plotted on Figure 10 are the density data obtained from the CTD profiles. Density variations with altitude are very small ($<2 \times 10^{-5}$ g/cm^3 over 700 m). More importantly, the transmission profile and density profile are found to have very little correlation. Intersection of transmission and density features indicates that turbidity variations do exist in an isopycnal environment and density variations occur in an isonepheloid environment. The transmission profiles cannot be explained by changes in the density profiles. In fact, the changes in density are minute, while transmission changes are quite large. The apparent density instability seen in Figure 10 is well documented by additional σ_t data taken within the same area (G. L. Weatherly, personal communication, 1980) and is a consequence of decreased salinity.

The results of the temporal and spatial transformations indicate that the Scotian Rise is an area in which large benthic clouds are formed hundreds of kilometers upstream and transported to the southwest remaining relatively unchanged. The measurements show that a profile of transmission at a given station represents what one should expect the profile to look like at a future time downstream. More importantly, it suggests that the major features (i.e., large benthic storms) detected optically are formed in a remote region and are transported along the topographic contours cohesively. Earlier it was suggested that the formation of smaller-scale features (e.g., detached benthic nepheloid layers) may be stimulated by small-scale (i.e., $\sim 10^2$ m) cross-slope effects. The large-scale features presently under discussion, however, appear to be formed upstream, and they resist significant changes as they move through the area.

The relationship of the large-scale features to gross topography can be further understood by considering maps of various bottom water parameters.

Figure 11 is a map of the bottom transmission values. Figure 12 is a similar map showing the thickness of the
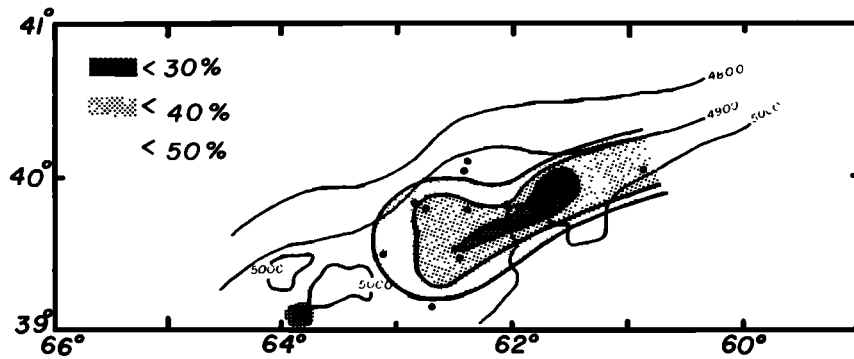
Fig. 11. Map of bottom contours and bottom transmission values.

bottom nepheloid layer in meters. Both figures demonstrate a southwest-northeast axis of alignment. In the transmission map (Figure 11) this is seen as the core of more turbid water, and in the thickness map (Figure 12) this is seen as the zone of the thickest bottom nepheloid layers. Clearer, thinner nepheloid layers are seen on either side of this core which lies roughly parallel to the bathymetric contours. Station 27 in the far southwest corner is characterized by very low bottom transmission (~0%) and a very thick bottom nepheloid layer (325 m). It is seen to lie just downstream of a large depression. Flow over the depression could yield a higher degree of turbidity and a much thicker nepheloid layer. Station 19 at the northeast corner has a high level of turbidity, which would classify it as being in the core; however, it is also defined by a very thin (60 m) benthic nepheloid layer and, consequently, is not considered part of the core as defined above. The explanation for this discrepancy is unclear. This may be a consequence of the small-scale local topography (e.g., depression or elevation affecting the flow), but the data do not exist to test this hypothesis. One cannot make a definitive statement relating the thickness of the bottom nepheloid layer to the magnitude of bottom turbidity; however, it is clear that there does exist a thick core of generally more turbid water flowing along the contours from the northeast to the southwest.

Conclusions

Vertical profiles of turbidity have been shown to be a useful parameter for the study of particle dynamics in the deep ocean.

Using the well-defined correlation of particle concentration and beam attenuation coefficient, a model was developed to describe quantitatively the transmissometer profiles.

The profiles were described by combinations of three components. Each component was of a simple mathematical form. Two of the components were shown to be representative of different physical systems. The physical explanation of the third component was ambiguous.

Both large-scale and small-scale processes were discovered to prevail in the temporal and spatial analysis of the optical data. The general scheme of transport was seen to be one combining turbulence and settling. It was shown that these two processes could explain the appearance of the most dominant components of the transmissometer profiles. By varying the magnitudes of either settling or advection, the shape of the profile was found also to vary accordingly. The other phenomenon observed directly from the vertical transmissometer profiles was the detachment of the benthic nepheloid layer. The detached benthic nepheloid layer was proposed to be probably due to cross-slope current-induced benthic layer detachment followed by transport along the contours by the dominant regional flow to the southwest. Due to the infrequency of cross-slope currents such a process cannot be considered common and, in fact, was detected in only several stations. The Eulerian transformation of the data produced a fixed-point time series representation of the profiles obtained over a wide area. The result was in good agreement with the time series obtained from the fixed-point in situ transmissometer used on the bottom ocean monitor. Similar 'storms' and clearing periods were detected with both techniques. Biscaye and Eittreim [1974] also detected periodic (~1 week) fluctuations in the turbidity structure of the benthic region of the Blake-Bahama Outer Ridge. These fluctuations were attributed to injections of colder, clearer Antarctic Bottom Water from the Hatteras Abyssal Plain. Such deflections were determined to be
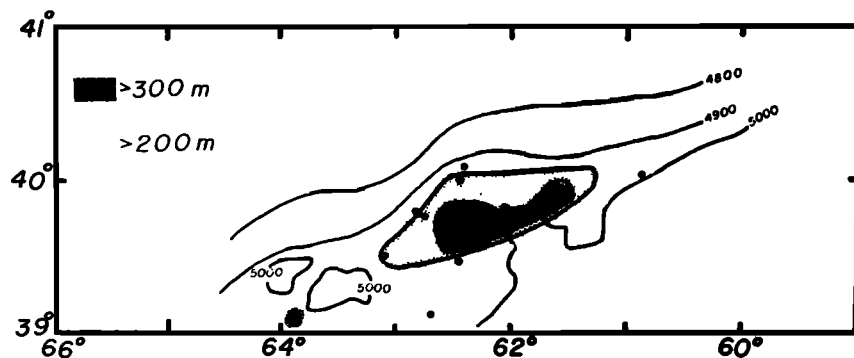

Fig. 12. Map of bottom contours and thickness of bottom turbid layer.

possibly influenced by local topography. Unfortunately, in the case of the measurements in the Scotian Rise there are no data regarding the optical characteristics of the benthic waters on the adjacent abyssal plain to determine if periodic injections from this region could explain the fluctuations in turbidity on the rise. Such a model should be considered in seeking the explanation for turbidity variability on the Scotian Rise. The Lagrangian transformation of the data yielded a section map of transmission at a given time. The widely varying bottom transmission values yielded little or no correlation between transmission and density (density was shown to be nearly constant at the bottom). Together, the temporal and spatial transformations of the data indicated that the major optical features detected in the HEBBLE area (i.e., large benthic clouds) were stable and nearly constant in form over periods of greater than 2 weeks and over distances traveled of several hundred kilometers.

Consideration of the transmissometer results obtained herein with deep-ocean optical data from elsewhere in the world yields some interesting comparisons. In general, bottom nepheloid layers of a similar nature to those in the Scotian Rise are found in regions characterized by high-velocity bottom currents. Highly turbid bottom nepheloid layers have been detected with nephelometers on the ridges and rises of the Canada Basin [*Hunkins et al.*, 1969], on the Blake-Bahama Outer Ridge [*Biscaye and Eittreim*, 1974], on the continental margin of the North American Basin [*Eittreim et al.*, 1969], in the Indian-Pacific Antarctic Sea [*Eittreim et al.*, 1972], and in the Cape Basin of the South Atlantic [*Connary and Ewing*, 1972]. Similarly, all of these regions are characterized by relatively high average bottom currents (of the order of 10^1 cm/s). Other benthic areas having lower or near-zero bottom velocities are not, generally, characterized by the intensely turbid benthic boundary layers. Examples are the Angola and Guinea basins [*Connary and Ewing*, 1972; *Zaneveld et al.*, 1979], the abyssal plains of the North Pacific [*Ewing and Connary*, 1970] and South Pacific [*Pak et al.*, 1979], and the Canada abyssal plain [*Hunkins et al.*, 1969].

It is the highly variable nature of the turbidity profiles that seems to be unique to the Scotian Rise. The component defined in this work by the sloping increase in turbidity near the bottom was also found in the continental rise of the North American Basin by *Eittreim et al.* [1969] as well as in the Indian-Pacific Antarctic [*Eittreim et al.*, 1972] and the Southeast Atlantic [*Connary and Ewing*, 1972]. The well-mixed linear component was seen in some nephelometer profiles made on the ridges within the Canada Basin [*Hunkins et al.*, 1969] and also in some of the deep basins of the Western North Atlantic [*Eittreim et al.*, 1972]. Near-bottom intermediate nepheloid layers (similar to the detached nepheloid layers discussed previously) are rarely seen and usually are only recorded hundreds of meters above the bottom in regions near topographic highs [*Pak et al.*, 1980a; *Eittreim et al.*, 1969].

Concluding, it appears that the optical profiles seem in the Scotian Rise contain features which are similar to features seen in separate turbidity profiles obtained in other deep-ocean areas of the world which are characterized by relatively strong benthic currents; however, the uniqueness of the Scotian Rise seems to lie in the diversity of profiles obtained. The other areas discussed indicate the wide range of turbidity profiles in areas with rough topography and strong bottom currents. The variations in turbidity within the same time

frame and spatial separation are much larger within the Scotian Rise than in any of the other areas cited.

REFERENCES

Armi, L., and E. D'Asaro, Flow structures of the benthic ocean, *J. Geophys. Res.*, *85*, 469, 1980.

Bartz, R., J. R. V. Zaneveld, and H. Pak, A transmissometer for profiling and moored observations in water, *Proc. Soc. Photo Opt. Instrum. Eng.*, *160*, 102–108, 1978.

Biscaye, P. E., and S. L. Eittreim, Variations in benthic boundary layer phenomena: Nepheloid layer in the North American Basin, in *Suspended Solids in Water*, edited by R. J. Gibbs, Plenum, New York, 1974.

Connary, S. D., and M. Ewing, The nepheloid layer and bottom circulation in the Guinea and Angola Basins, in *Studies in Physical Oceanography*, vol. 2, edited by A. L. Gordon, Gordon and Breach, New York, 1972.

Eittreim, S., M. Ewing, and E. M. Thorndike, Suspended matter along the continental margin of the North American Basin, *Deep Sea Res.*, *16*, 613, 1969.

Eittreim, S., A. L. Gordon, M. Ewing, E. M. Thorndike, and P. Bruchhausen, The nepheloid layer and observed bottom currents in the Indian-Pacific Antarctic Sea, in *Studies in Physical Oceanography*, vol. 2, edited by A. L. Gordon, Gordon and Breach, New York, 1972.

Ewing, M., and S. D. Connary, Nepheloid layer in the North Pacific, *Mem. Geol. Soc. Am.*, *126*, 41–82, 1970.

Hollister, C. D., A. R. M. Nowell, and J. D. Smith, The third annual report of the High Energy Benthic Boundary Layer Experiment, *Rep. 80-32*, Woods Hole Oceanogr. Inst., Woods Hole, Mass., 1980.

Hunkins, K., E. M. Thorndike, and G. Mathieu, Nepheloid layers and bottom currents in the Arctic Ocean, *J. Geophys. Res.*, *74*, 6995, 1969.

Jerlov, N. G., *Marine Optics*, Elsevier, Amsterdam, 1976.

Pak, H., D. Menzies, and J. R. Zaneveld, Optical and hydrographical observations off the coast of Peru during May–June 1977, *Ref. 79-14*, Oreg. State Univ., Sch. of Oceanogr., Corvallis, 1979.

Pak, H., L. A. Codispoti, and J. R. Zaneveld, On the intermediate particle maxima associated with oxygen-poor water off Western South America, *Deep Sea Res.*, *27*, 783, 1980a.

Pak, H., J. R. V. Zaneveld, and J. Kitchen, Intermediate nepheloid layers observed off Oregon and Washington, *J. Geophys. Res.*, *85*, 6697, 1980b.

Raudkivi, J., *Loose Boundary Hydraulics*, Pergamon, Oxford, 1967.

Shepard, F. P., *Submarine Geology*, 2nd ed., Harper and Row, New York, 1963.

Smith, J. D., and S. R. McLean, Spatially averaged flow over a wavy surface, *J. Geophys. Res.*, *82*, 1735, 1977.

Spinrad, R. W., Optical characteristics of the suspended sediment in the high energy benthic boundary layer experiment, Ph.D. thesis, Oreg. State Univ., Corvallis, 1982.

Spinrad, R. W., and J. R. V. Zaneveld, An optical study of the suspended particles in the benthic nepheloid layer of the Scotian Rise, *Mar. Geol.*, in press, 1982.

Weatherly, G. L., E. A. Kelley, J. R. V. Zaneveld, H. Pak, M. J. Richardson, and M. Wimbush, A deep, narrow, thin filament of the western boundary undercurrent (WBUC), *Eos. Trans. AGU*, *61*, 1016, 1980.

Zaneveld, J. R. V., R. W. Spinrad, and D. W. Menzies, Optical and hydrographic observations in the Congo River and Angola Basin during May 1978, *Ref. 79-3*, Oreg. State Univ., Sch. of Oceanogr., Corvallis, 1979.